Gould, J. W., and F. M. Kenyon, "Gas Discharge and Electric Field Strength in Microwave Freeze-Drying," *J. Microwave Power*, 6(2), 151 (1971).
Harper, J. C., "Transport Properties of Gases in Porous Media at Reduced Pressures with Reference to Freeze-Drying," *AIChE J.*, 8, 298 (1962).
Hill, J. E., and J. E. Sunderland, "Sublimation in Dehydration in the Continuum, Transient and Free-Molecule Flow Regimes," *Intern. J. Heat Mass Transfer*, 14, 625 (1971).
Hill, J. E., J. D. Leitman, and J. E. Sunderland, "Thermal Conductivity of Various Meats," *Food Technol.*, 21, 1143 (1967).
Hohner, G. A., *An Analysis of Heat and Mass Transfer in Atmospheric Freeze-Drying*, Ph.D. thesis, Mich. St. Univ., East Lansing (1970).
Hoover, M. W., A. Markantonatos, and W. N. Parker, "UHF Dielectric Heating in Experimental Acceleration of Freeze-Drying of Foods," *Food Technol.*, 20, 103 (1966).
———., "Engineering Aspects of Using UHF Dielectric Heating to Accelerate the Freeze-Drying of Foods," *ibid.*, 107 (1966).
Jackson, S., S. L. Rickter, and C. O. Chichester, "Freeze-Drying of Fruit," *Food Technol.*, 11, 468 (1957).
Kan, B., and R. A. Yeaton, "Improving Freeze-Drying Process Efficiency through Improved Vapor Removal and In-Process Moisture Determination," QM Contract Report, DA 19-129-QM-1546 (1961).
King, C. J., *Freeze-Drying of Foods*, CRC Monoscience Series, (1971).
Lentz, C. P., "Thermal Conductivity of Meats, Fats, Gelatin Gels and Ice," *Food Technol.*, 15, 243 (1961).
Ma, Y. H., and P. Peltre, "Mathematical Simulation of a Freeze-Drying Process Using Microwave Energy," AIChE Symp. Ser. *No. 132*, 69, 47 (1973).
———., "Freeze Dehydration by Microwave Energy: Part II. Experimental Investigation," *AIChE J.*, 21, 344 (1975).
Miller, H. L., and J. E. Sunderland, "Thermal Conductivity of Beef," *Food Technol.*, 17, 124 (1963).
Peltre, P., *Freeze-Dehydration by Microwave Energy*, Ph.D. thesis, Worcester Polytechnic Inst. Mass. (1974).
Rey, L., *Aspects Théoriques et Industriels de la Lyophilisation*, Herman, Paris (1964).
Sandall, C. C., C. J. King, and C. R. Wilke, "The Relationship Between Transport Properties and Rates of Freeze-Drying of Poultry Meat," *AIChE J.*, 13, 428 (1967).
Therlkeld, J. L., *Thermal Environmental Engineering*, Prentice Hall, Englewood Cliffs, N. J. (1962).
Wakao, N., S. Otani, and J. M. Smith, "Significance of Pressure Gradients in Porous Materials: Part 1., Diffusion and Flow in Fine Capillaries: Part 2., Diffusion and Flow in Porous Catalysts," *AIChE J.*, 11, 435 (1965).

Manuscript received August 21, 1974; revision received December 26, 1974, and accepted January 2, 1975.

Freeze Dehydration by Microwave Energy:

Part II. Experimental Study

Experimental drying curves have been obtained for the freeze-dehydration of beef meat with microwave energy at 2450 MHz. In particular, experiments conducted with slabs of raw beef meat approximately 1.5 cm thick show that total drying times of less than 6 hr. can be obtained. Further drying time reductions are possible if microwave heating and freezing techniques are improved. Samples can be dried slightly faster at a higher pressure (for example, 1 mmHg) than at a lower pressure (for example, 0.2 mmHg) for the same microwave power input. However, melt back and vaporization occur if the pressure or the microwave power input is too high.

Comparison of the experimental drying curves with those predicted by the theory shows a reasonable agreement which, at least in part, verifies the validity of the previously derived mathematical model.

YI HUA MA

and

PHILIPPE R. PELTRE

Department of Chemical Engineering
Worcester Polytechnic Institute
Worcester, Massachusetts 01609

SCOPE

Although freeze drying is normally considered to be a slow process, the acceleration of the process can be achieved by the application of volumetric heating (for example, microwave energy) as previously demonstrated (Jackson et al., 1957; Copson, 1958). Previous work concentrated mostly in demonstrating the feasibility of microwave energy for freeze drying. A detailed theoretical investigation with a verification by an experimental study is lacking.

The present work employed an experimental multimode cavity to investigate the freeze-dehydration of beef meat at a microwave frequency of 2450 MHz. Utilization of a specially designed continuous weighing system provided a means of investigating the effects of the microwave power input and the total pressure of the vacuum upon the drying rate. Melt back of the sample at high microwave power input and at high pressure in the vacuum chamber was observed. Comparison of the experimental drying curve with those predicted by the model previously developed by the authors (Peltre, 1974; Ma and Peltre, 1975) showed a good agreement between the experimental and theoretical results.

Correspondence concerning this paper should be addressed to Y. H. Ma. P. R. Peltre is with the U.S. Army Natick Laboratories, Natick, Massachusetts.

CONCLUSIONS AND SIGNIFICANCE

Drying curves of beef samples have been obtained experimentally by freeze-dehydration with microwave heating at 2450 MHz. These experiments are primarily intended as a verification of a theory derived by the authors (Peltre, 1974; Ma and Peltre, 1974). The experimental drying curves are in good agreement with those predicted by the theory. The small differences observed may be due to an uncertainty on the value of the numerical data (particularly diffusivity and dielectric properties) used in the calculations or to nonideal experimental conditions, for example, nonuniform electric field distribution in the sample, nonconstant standing wave pattern in the cavity or nonuniform thickness of the sample.

The startup portions of the experimental drying curves have been utilized to determine the value of the heat transfer coefficient (1.9×10^{-4} cal/cm^2-s-°C) at the outer surface of the sample (drying on both sides). Use of this value gave excellent agreement between the predicted and experimental startup portions of the drying curves.

The difference between the theoretical (170V/cm) and experimental (125V/cm) electric field peak strength (in the vacuum) at which melt back starts to occur seems to reflect experimental heating nonuniformities. However, it may also partially indicate that the actual diffusivity in the experiments is somewhat lower than that assumed in the calculations.

Thus, considering the generally good agreement between theory and experiments, it seems that the model derived by Ma and Peltre (1975) can be utilized to simulate with good accuracy the sublimation dehydration process with microwave heating provided that adequate numerical data are available and that near uniform heating conditions can be realized.

Experimental investigations dealing with microwave freeze drying concentrate mostly in demonstrating the feasibility of the process. Jackson et al. (1957) and Copson (1958) successfully accelerated freeze drying with microwave energy and found that microwave heating should allow a drastic reduction of the drying time although engineering problems, particularly glow discharge, may complicate its application. Harper (1961) and Kan and Yeaton (1961) obtained experimental data on the dielectric properties of various food products between microwave frequencies of 500 to 3000 MHz. Hoover et al. (1966) obtained comparative drying curves for radiant and microwave (at 632 and 915 MHz) freeze drying of various food products. They demonstrated that use of microwave heating may reduce drying times by factors of 3 to 13 as compared to radiant (surface) heating. They observed that with microwave heating drying times of about 2-1/2 hr. for beef patties of various thicknesses were obtained. The drying times were essentially independent of the thickness of the sample. It should be noted that the microwave power input level was increased in their experiments in the same ratio as the thickness. They also reported variations of the glow power vs. pressure for the microwave applicator which they used. In a succeeding paper (Hoover et al., 1966) they used engineering data derived from their experimental results to discuss the feasibility of the microwave freeze-drying process. More recently, Gouigo et al. (1969) have reported experiments in which they accelerated freeze-drying with microwaves at 2450 MHz and obtained drying times of 20 to 30 min. for meat samples 6 to 7 mm thick.

A principal objective of the present investigation is to provide experimental data on microwave freeze drying for the verification of the previously derived mathematical model. Freeze dehydration of beef meat at a microwave frequency of 2450 MHz was chosen for the study. Effects of microwave energy inputs and the pressure in the vacuum chamber upon the freeze-drying rate were investigated.

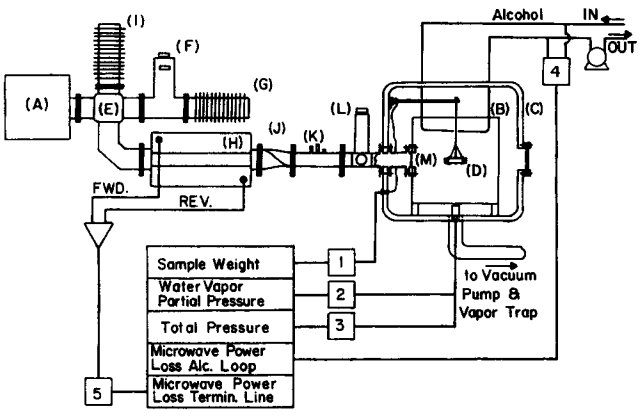

Fig. 1. Schematic of the experimental setup.

EXPERIMENTAL SETUP AND PROCEDURE

Apparatus

A schematic of the experimental system is given in Figure 1. The microwave generator (A) is a converted microwave oven (Speed Range 110) which uses a magnetron Amperex DX-206 to deliver 1.2KW of adjustable power at 2450 MHz ± 25 MHz. The microwave applicator cavity (B) is located inside a vacuum chamber (C) and contains the sample to be dried (D). The microwave power is transmitted to the cavity (B) by a rectangular wave guide WR-284, through various control, monitoring, and tuning devices. The power from the generator is sent by a four-port circulator (E) into the line section where an H-tuner (F) varies the admittance to a dry resistor (G). The fraction of power reflected at the H-tuner travels back to the circulator where it is diverted into the termination line section (microwave applicator and freeze dryer). It encounters a bidirectional coupler (H) which separates the power traveling forward from that traveling reverse (reflected from the termination). The reverse power travels back to the circulator where it is sent to a second dry resistor (I) in order to prevent harmful reflections to the magnetron. The bidirectional coupler is connected to a twist (J) which rotates 90° the original polarization of the electric field. The electric field enters the cavity (B) with a vertical polarization (parallel to the figure plane). A 3-Stub tuner (K) is used in conjunction with an E-H tuner (L) to tune the cavity (B). The microwave power enters the cavity (B) through a wave guide vacuum transition (M)

using a fiber glass window.

The multimode rectangular cavity (B) has dimensions 39 × 39 × 51 cm and is made of perforated aluminum sheets in order to retain the microwave power but let the water vapor from the dehydration flow through to the main chamber (C) and finally the vapor trap. An oversized condenser is used for the vapor trap. The sample to be freeze dried (D) is hung inside the cavity (B) with its main surface horizontal and is located in front of the wave guide mouth as shown in Figure 1. It is suspended to a cantilever beam, used in the weight measuring system, by means of teflon hooks and fiber glass strings.

Finally, *n*-propyl alcohol is circulated at a constant flow rate in a glass loop inside the cavity. It was intended to serve a double purpose. First, in order to obtain a fairly uniform field in the multimode cavity, a reasonable load is necessary. By increasing the load, one decreases the Q of the cavity and broadens its frequency band at resonance. Thus, more modes (eigen frequencies) can be admitted inside the cavity which superimpose and average out to yield a relatively uniform field. The increase of the load was found necessary, due to the small size of the sample used (about 60 to 90 cm^3) as compared to the large volume of the cavity (about 7.5×10^4 cm^3). *n*-propyl alcohol was chosen as the circulating fluid because of its dielectric constant ($\epsilon' = 3.7$) comparable to that of frozen beef meat ($\epsilon' = 3.6$). Second, it was intended as a means of qualitative monitoring of the electric field inside the cavity.

The sample is suspended by means of a fiber glass string to the free end of a cantilever beam through a knife edge as shown in Figure 1. The strain induced at the fixed end by the sample weight is measured by four strain gauges mounted in a Wheatstone bridge. The DC signal resulting from the unbalance of the bridge in the measuring circuit, when the sample is hung, is amplified and sent to a strip chart recorder. Known weights are used to calibrate the measuring system. A filter, specially designed for the purpose, was necessary to suppress the electrical noise in the output of the DC amplifier, which was caused by mechanical vibrations induced in the beam by surrounding machinery. The assembly (DC power supply, balancing unit, DC amplifier, filter and strip chart recorder) is referred to in Figure 1 as data acquisition unit 1. The water vapor partial pressure in the vacuum chamber is measured continuously by a Panametrics model 1000 hygrometer (unit 2).

The total pressure is monitored by a MacLeod Pressure gauge (unit 3) equipped with a vapor trap. The microwave power loss in the alcohol is determined from the temperature difference between the inlet and the outlet measured with a Doric digital thermocouple temperature indicator (unit 4).

The total microwave power loss in the termination line (including twist, tuners, window, connectors, leakage, sample, and alcohol) is measured from the forward and reverse microwave powers detected in the bidirectional coupler. The detected forward and reverse powers are determined by a Hewlett-Packard 431 B power meter which uses a thermistor mount (unit 5). However, due to the relatively high fraction of power lost in leakage, the results of the power measuring unit were limited to comparisons between runs.

Sample Preparation

Two batches of samples of different choices of raw beef meat with different preparation were used. The first one, used in the study of the effects of the power input on the drying curves, consisted of an eye of the round choice which offers a rather homogeneous fat free texture (moisture: 71%). The outer fat was trimmed and the meat deep frozen in a blast freezer to approximately −37°C. Slabs of approximately 1.5-cm thickness were cut perpendicularly to the fibers from the frozen muscle with an electric band saw. The samples were then wrapped separately and stored in a freezer until later use. However, there were two drawbacks to this method of preparation. The thickness and the contour of the slab were irregular and difficult to reproduce. Thus another preparation method was employed in the study of the effects of pressure on the drying curves. However, since a larger muscle cross section was needed, a different choice of meat was used. It consisted of top of the round (average moisture: 67%, average fat: 2%) The whole muscle was tempered at about −3°C and then pressed and formed in a cylindrical die, with the general orientation of the fibers parallel to the cylinder axis. The meat cylinder was then chopped automatically in slabs of a relatively constant thickness (approximately 1.5 cm). 7.5-cm diameter disks were then punched out of the meat slab with a metal cutting form and placed on a metal tray and refrozen in a blast freezer. It should be noted that the freezing method does not seem adequate since the fast freezing from the bottom of the sample resting on the tray yields a concave top surface. A different method might have given better results. The frozen samples were again wrapped separately in paper and stored in a freezer at about −37°C.

Experimental Procedure for a Run

Before each series of runs, tuning of the cavity was necessary in order to obtain a relatively uniform electric field. The uniformity of the field was checked on a test run by visual examination of a partially dried sample cut in several directions. A planar ice-front was usually observed, which indicated a relatively uniform heating.

Before each run, a known weight was suspended from the cantilever beam in place of the sample and the reading of the weight on the recorder was allowed to reach a constant value. This normally took one to two hours. Once the reading was constant, the gain of the recorder was adjusted for a direct reading in grams. The refrigeration system and vacuum pump were started 30 min. to 1 hr. prior to each run with the vacuum chamber isolated in order to achieve a constant condenser temperature of approximately −40°C.

The meat sample was then taken from the storage freezer, weighed, and its cross section area and thickness were measured. The sample was then attached to the fiber glass string from the cantilever beam weighing system by means of three teflon hooks, its surface horizontal and its edge facing the mouth of the microwave power feed (wave guide). Thus, the polarization of electric field at the sample surface was expected to be mainly that in the wave guide ($TE_{1,0}$), that is, vertical (normal to the sample surface).

The doors of the microwave cavity and vacuum chamber were then shut and the chamber opened to the vacuum. The desired vacuum was reached in less than 5 min.

Usually after 30 min. (startup period) the microwave power was turned on. The desired power input was selected by using the H-tuner (F in Figure 1). The sample was then allowed to dry. It was considered fully dried when the weight reading on the recorder reached a constant value. The drying curve (sample weight vs. time) was directly given by the reading on the strip chart recorder.

It should be noted that in certain instances, especially during the runs at high pressure (3.5 mmHg), a corona discharge occured at the end of the dehydration. The high pressure runs (3.5 mmHg) were not relevant due to local melting and vaporization of the frozen core. Otherwise, a corona-free operation was reached.

RESULTS AND DISCUSSION

Experimental Results

Drying curves have been obtained at various microwave power inputs for a constant vacuum pressure of approximately 0.3 mmHg (referred to as *power runs*) and at various pressures for a fixed microwave power input (referred to as pressure runs) corresponding to an electric field peak strength of about 125 V/cm in the vacuum.

Two different batches of raw meat samples were used for the power and pressure runs. An eye of the round choice of meat was used for the power runs, while the pressure runs were performed with top of the round. The two batches further differed by the geometry of the slabs and the preparation of the sample as discussed previously. It should be noted that the thickness of the slabs was not uniform for any sample and varied between different samples due to difficulties in their preparation. A variation of 1 to 2 mm about the mean thickness (approximately 1.5 cm) was observed for a sample.

Table 1 shows the operating conditions used for each run the average value used to calculate the theoretical dry-

TABLE 1. EXPERIMENTAL CONDITIONS

Run number	$E^a_{exp.}$ V/cm	P_R mmHg	$P_R{}^w$ mmHg	L cm	x_w —	$\frac{m_1 - m_f}{m_0 - m_f}$ —	$h^b \times 10^4$ cal/cm² s/°C	t_1 min	Type
25	125	1.0	0.4	0.8	0.66	0.923	2.1	30	
27	125	0.2	0.2	0.8	0.69	0.944	1.6	30	Pressure
29	125	3.5	0.5	0.75	0.67	0.952	1.4	30	Runs
Average	125	NA	NA	0.78	0.67	0.94	1.7	30	
12	103	0.32	0.23	0.71	0.71	0.957	1.3	24	
13	107	0.29	0.27	0.74	0.72	0.950	—	19	
14	145	0.24	0.23	0.71	0.70	0.905	1.9	35	
15	125	0.30	0.30	0.78	0.72	0.936	2.1	30	Power
16	135	0.31	0.30	0.76	0.71	0.941	2.3	30	Runs
17	120	0.27	0.26	0.71	0.71	—	—	—	
Average	NA	0.29	0.26	0.735	0.71	0.94	1.9	NA	

[a] Estimated from drying curve.
[b] Estimated from startup portion of drying curve.

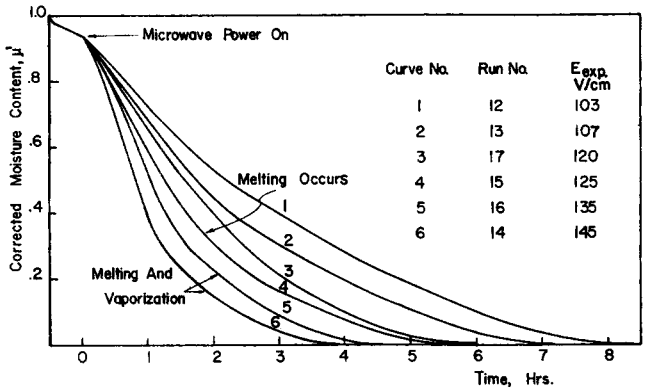

Fig. 2. Experimental drying curves (power runs). $P_R = 0.3$ mmHg.

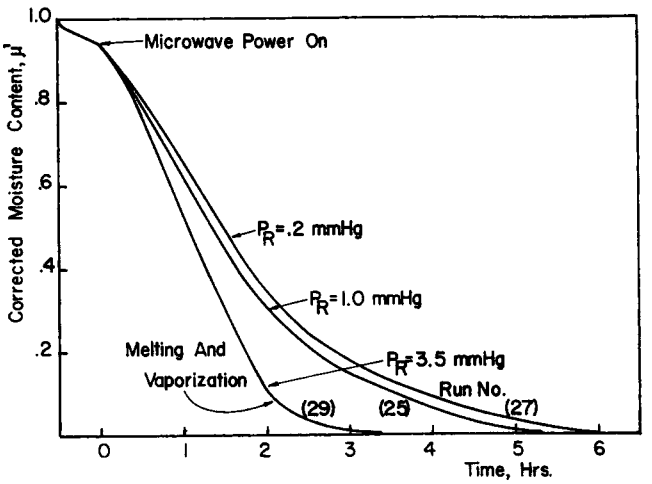

Fig. 3. Experimental drying curves (pressure runs).

ing curves. The values given for the total pressure and partial pressure of water vapor correspond to the starting point when the microwave power is turned on. They decreased slowly during most of the drying (a drop of about 0.05 to 0.1 mmHg) and relatively faster in the final stage during which an additional drop of approximately 0.05 mmHg was observed. The initial temperature is not given as it was not possible to measure it directly from the sample when enclosed in the microwave oven. The results from the theoretical study have shown (Ma and Peltre, 1975; Peltre, 1974) that the starting temperature is not a significant parameter of the process.

Assuming that the variations of the sensible heat of the sample and the heat losses to or from the surrounding atmosphere were negligible compared to the microwave power absorbed in the sample, the electric field strength in the vacuum (near the sample surface) was estimated from the drying rate. With this assumption the power dissipated by the microwave field in the sample could be equated to that consumed by the sublimation:

$$\Phi_T = \Phi_F + \Phi_D = \Delta H_s \dot{m} \tag{1}$$

where the total microwave power dissipated Φ_T can be further related to the electric field strength by

$$\Phi_T = [K_F(T_F)V_F + K_D(T_D)V_D]E^2 \tag{2}$$

The *dissipation coefficients* K_F and K_D which are functions of the temperature were estimated from the numerical data shown in Part I, Figures 2 and 3 by assuming an average temperature for the frozen region and the dry layer. The volumes V_F and V_D of the frozen and dried portions were determined using the interface position derived from the drying curve at the point where the calculations were made (usually half dehydration point and/or maximum of the drying rate curve). An average 16% shrinkage (as observed experimentally) was further allowed for the determination of the volume of the dry layer. Table 1 shows the results of the calculations for the electric field peak strength in the vacuum.

The starting fraction of the initial moisture content $\mu_1 = (m_1 - m_f)/(m_0 - m_f)$ (corresponding to the time when the microwave power is turned on) varied from one run to the other due to difficulties in reproducing the operating conditions. Thus, the microwave drying curves have been first normalized to permit their comparison. The normalized values were then corrected to the average starting fraction of the initial moisture content ($\mu_1 = 0.94$) to include the startup stage of the process under average operating conditions. Thus, the following quantity:

$$\mu' = \frac{m - m_f}{m_1 - m_f}\,\mu_{1,\text{aver.}} \tag{3}$$

has been plotted vs. time in Figures 2 and 3. The average value of μ_1 observed for both the pressure and the power runs is 0.94. Typical startup portions of the drying curve have been plotted in Figure 2 using data of Run 16 and Figure 3 using data of Run 27.

Figure 2 shows the drying curves obtained at various

electric field strengths for an average chamber pressure of 0.3 mmHg. The common portion during the startup stage of the process (before the microwave power is turned on) and exhibits the same characteristics as that predicted by the theory (Figures 7 and 8, Part I). An initially high drying rate exists as the dry layer is very small and the mass transfer driving force high due to the low partial pressure of vapor in the vacuum. It decreases rapidly as the temperature of the frozen material drops to the wet-bulb temperature of the vacuum and becomes practically constant until the microwave power is turned on. This reflects the wet bulb process which takes place. The drying rate starts to increase as microwave energy is absorbed in the sample.

It can be seen from Figure 2 that the drying rate increases substantially when the electric field strength is increased as expected from the theory. Toward the end of the drying the curves start to level off. This corresponds to the stage in which the frozen core has disappeared and the residual adsorbed moisture is being removed from the dried product. In some applications, this latter stage is usually of little interest as only removal of the frozen moisture content is sought. The residual moisture content can be determined from a plot of the drying rate vs. time as the curve exhibits a sudden decrease of the slope when the frozen core disappears. This is shown in Figure 4. It has been found by this technique that the residual moisture content is less than 5% of the initial sample weight or 7% of the initial weight of water. The final residual moisture content was found to be approximately 1.5% of the initial sample weight for all runs except Runs No. 12 and 15 for which it was about 4.5%. This is reflected on Figure 2 by the early leveling off of the corresponding drying curves.

It should be noted that a visual examination of the dried sample obtained in Run No. 13 showed local burns of the material which indicated a nonuniform field distribution for this run. The tuning of the cavity was readjusted following this run and the problem was corrected.

When a higher microwave power is used, melting of the frozen material starts to occur (Run No. 15), followed by a local vaporization (Runs No. 16 and No. 14). The local vaporization indicates that the dielectric heating is not perfectly uniform although a relatively planar ice-front has been observed at medium and low power levels (by cutting in different directions a partially dried sample). It seems that for the lower power input, the drying rate is small enough to permit the temperature nonuniformities in a cross section to level out. This is less likely to occur at the higher power levels. Thus, a nonplanar ice-front and hot spots may develop in the frozen region inducing an early melting of the frozen core.

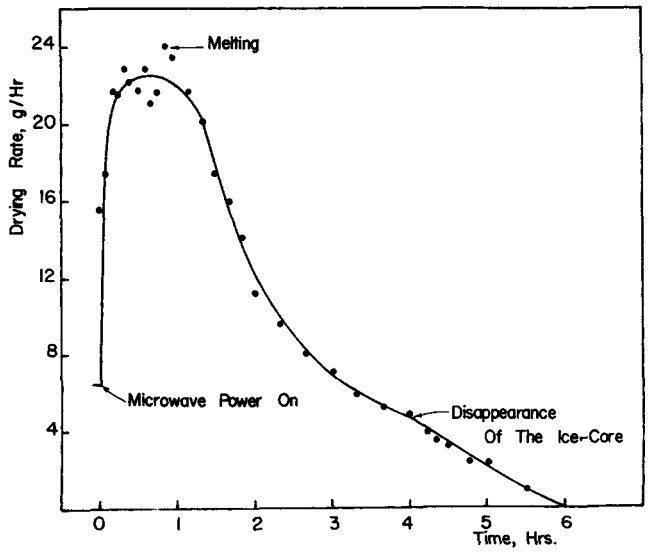

Fig. 4. Drying rate vs. time, Run No. 15.

Melting is believed to start occurring with Run No. 15 as the drying rate exhibits (Figure 4) a sudden increase at time $t = 0.8$ hr. This was confirmed during the experiments by the observed drop of the microwave power loss in the alcohol loop as the power input was kept constant. Indeed, as a higher microwave power is used (Run No. 16 and No. 14) local vaporization takes place. As the ice melts and vaporization occurs, a much higher drying rate develops locally due to the higher dissipation factor of the wet material. This phenomenon can also be observed visually as a dark spot and puffing develop at the surface of the sample.

Figure 3 shows similar plots for the drying curves at various pressures and a fixed microwave power input. An electric field peak strength of 125 V/cm has been estimated for the three runs by the method outlined earlier. It can be seen from this figure that the sample dried faster for a pressure of 1 mmHg than for 0.2 mmHg as expected from the theory (Ma and Peltre, 1974). This can be explained by the increase of the dissipation coefficient with the temperature, mainly in the frozen core, due to the higher resistance to mass transfer in the dry layer. In fact, when the pressure of the vacuum chamber is increased to 3.5 mmHg, melting of frozen core occurs early during the dehydration and is followed by a local vaporization.

Comparison Between Experimental and Simulated Drying Curves

In order to obtain theoretical drying curves for comparison with those obtained experimentally, the heat transfer coefficient has been estimated from the startup portion of the drying curves (just before the microwave power is turned on). This was done by assuming a linear temperature profile in the dry layer. The frost-point temperature corresponding to the partial pressure of water vapor in the vacuum chamber was used to approximate the ice-front temperature (actually equal to the wet-bulb temperature of the vacuum) as the drying rate was small. It can be seen from an energy balance on the dry layer that

$$h(T_R - T_{s,1}) = k_D \frac{T_{s,1} - T_{i,1}}{\delta_1} = Q_{s,1} = \Delta H_s W_1 \quad (4)$$

h can then be related to the drying rate before the microwave power is turned on by

$$h = \Delta H_s \frac{1+\beta}{T_R - T_{i,1}} W_1 \quad (5)$$

where β is given by

$$\beta = \text{Biot number} = \frac{h\delta_1}{k_D}$$

and δ_1 is the dry layer thickness.

Values of h calculated in this manner are shown in Table 1 for each run. The average value of 1.9×10^{-4} cal/cm^2-s-°C found for the first batch (eye of the round) was used in the simulation. Due to the concave shape of the slab in the second batch, the thickness of the dry layer could not be determined accurately. Thus, this might result in a higher uncertainty on h.

In order to compare the theoretical curves with experimental values, the experimental drying curves were modified to represent the variations of the ice-front position with time. In effect, the normalized ice-front position (Peltre, 1974) can be related to the weight loss by

$$S(t) = \frac{m(t) - (m_f + m_r)}{m_0 - m_f} = \frac{m(t) - m_f}{m_0 - m_f} - \frac{m_r(t)}{m_0 - m_f} \tag{6}$$

m_r is the weight of residual water adsorbed in the dry layer, and $m_r/(m_0 - m_f)$ the fraction of adsorbed moisture.

Since $m_r(t)$ was not known it was estimated from its final value $m_{r,2}$ assuming a linear variation with time. $m_{r,2}$ was obtained from the drying rate curves (such as Figure 4). The following formula was used to determine the position of the interface at any time from the experimental drying curves:

$$S(t) = \frac{m(t) - m_f}{m_0 - m_f} - \frac{m_{r,2}}{m_0 - m_f} \cdot \frac{t}{t_2} \tag{7}$$

Results from the computer simulation (using the average operating conditions of the power runs—see Table 1) gave the melting occurrence at an electric field peak strength of 170 V/cm. However, an experimental value of approximately 125 V/cm (Figure 2) was observed. Although this discrepancy most likely could be attributed experimentally to a nonuniform heating, it was felt that the diffusivity values used in the calculations might have been overestimated. This may be due to the fact that turkey diffusivity values were used as diffusivity data for beef meat were not available. On the other hand, significant variations of D can be expected depending on the choice of meat and most of all the rate of freezing as different ice formations

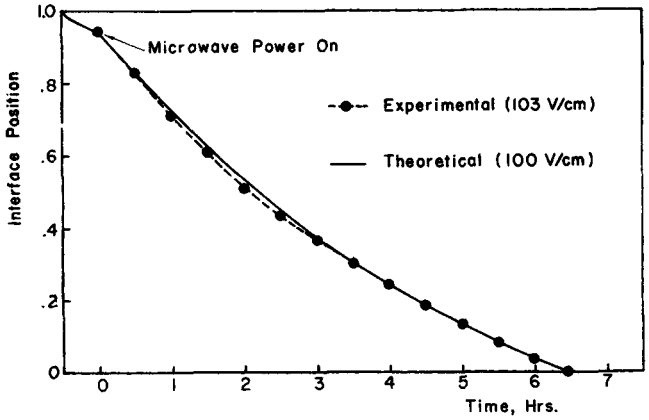

Fig. 5. Experimental (Run No. 12) and simulated drying curves. $P_R = 0.3$ mmHg.

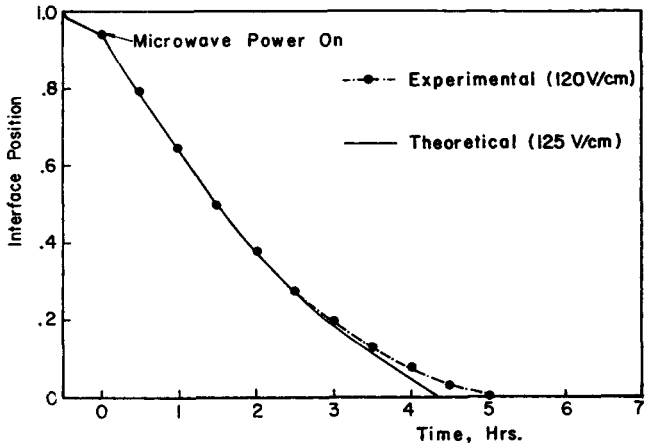

Fig. 6. Experimental (Run No. 17) and simulated drying curves. $P_R = 0.3$ mmHg.

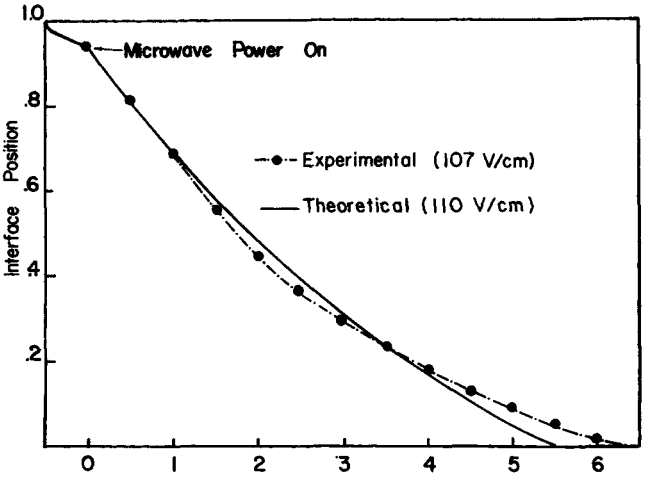

Fig. 7. Experimental (Run No. 13) and simulated drying curves. $P_R = 0.3$ mmHg.

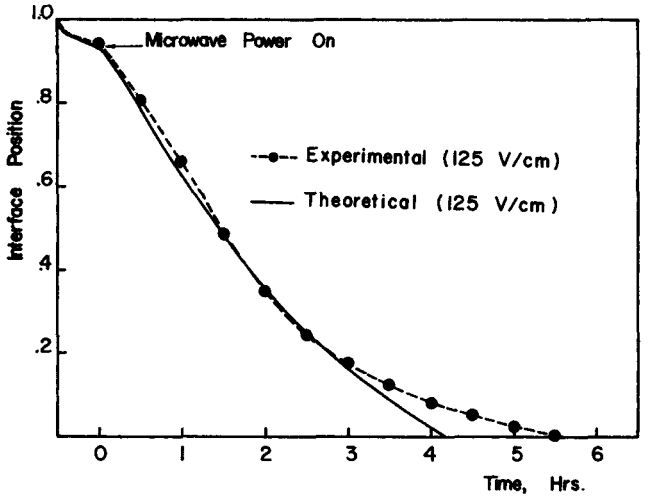

Fig. 8. Experimental (Run No. 27) and simulated drying curves. $P_R = 0.2$ mmHg.

are obtained. Indeed, when slow controlled freezing rates are used, big ice crystals form in the meat outside the cells. The resulting wide channel structures facilitate the water vapor flow during freeze drying. In other words, a higher diffusivity is obtained in this case. It is believed that the reasons why drying times obtained from this study (for example, drying time for a 1.5 cm thick raw beef slab was 5-1/2 hr.) are larger than those obtained by Hoover et al. (1966) for example, drying time for a 1.27-cm thick chopped beef patty was 2-1/2 hr.) may be experimental nonuniform heating, variations of diffusivity with choice of meat and the rate of freezing.

Figures 5 through 8 show plots of the variations of the interface position determined from the experimental results by Equation (7). The theoretical curves predicted by the simulation are also shown in these figures. The theoretical drying curves were calculated using the average operating conditions (shown in Table 1) by the model described in Part I (variable properties). The electric field strengths used in the simulation were adjusted in order to give the best fit. Ideally, the comparison should be made by comparing predicted and experimental drying curves using the same input operating conditions. However, to the best of our knowledge, there is no known way to measure directly the E field strength in a microwave cavity at the power level used. Thus, E was estimated by Equations (1) and

(2) from the drying rate observed experimentally. Unfortunately, under this circumstance, although the estimated E value may be accurate, it is known with a relatively low level of confidence. Thus, an alternative way to test the model is to adjust the E value (to which results are known to be very sensitive) such that the experimental and theoretical curves agree. An agreement between E value used in the calculation and that determined in the experiments certainly provides an indication that the model is realistic. It should be noted that only one adjustable constant is used.

The final values of the electric field strength used to calculate the curves shown in Figures 5, 6, 7, and 8 agree within 4% or less of those determined experimentally. A good agreement is also found between the theoretical and experimental drying curves as shown by Figures 5 and 6. The small differences observed may just be the inherent differences between the model and the experiments. However, they may also reflect an uncertainty in the numerical data used in the model (especially diffusivity and dissipation coefficient) or nonideal experimental conditions, for example, nonuniform field distribution in the sample; nonconstant standing wave pattern in the cavity; nonuniform thickness of the sample.

The possibility for a nonuniform field is indicated by the local vaporization which occurred in Runs No. 14 and 16, and the local burns of the sample observed in Run No. 13. It may explain the discrepancy observed for this latter run between simulated and experimental drying curves (Figure 7). Indeed the sudden decrease of slope in Figure 7 of the experimental drying curve with respect to the theoretical one was found to correspond to a peak of the experimental drying curve which may have been caused by a local melting. Thus, a nonuniform field distribution in the sample may have caused the smaller differences observed tbetween theoretical and experimental curves in Figure 6 toward the end of drying.

Figure 8 constitutes another example of a case where a strong nonideality is known to exist. As already mentioned earlier in this paper, the thickness of the sample was not uniform due to the concave top surface which was caused by the freezing method. The thickness of this sample varied by as much as 0.6 cm from edge to center compared to a thickness at the edge of approximately 1.3 cm. This is approximately a 50% variation. It is believed that the nonuniformity of the thickness may be the cause for the discrepancy observed in Figure 8 between simulated and experimental drying curves.

However, the good agreement obtained between the simulated and experimental drying curves in the runs where near ideal conditions are believed to have prevailed (Figures 5 and 6) seems to demonstrate that the mathematical model derived is realistic and can be used to simulate the microwave freeze-drying process.

It should be mentioned that the application of some of the literature data on the properties of beef in the case investigated may be somewhat questionable. Indeed, more specific and comprehensive data on the properties (particularly diffusivity and dielectric properties) have to be obtained before the model can be used for effective simulation of the process. More experimental information still has to be obtained on the microwave freeze-drying process for a complete verification of the predictions of the model.

ACKNOWLEDGMENT

This research is supported by the U.S. Army Natick Laboratories through Grant DAAG 17-71-G-01. Use of the facilities of the Worcester Area College Computation Center is gratefully acknowledged.

NOTATION

E = electric field peak strength in the vacuum, V/cm
h = heat transfer coefficient, cal/s-cm^2-°K
ΔH_s = enthalpy of sublimation, cal/g
k = effective thermal conductivity, cal/s-cm-°K
K = dissipation coefficient as defined by Ma and Peltre (1975), cal/s-cm^3-(V/cm)^2
L = sample half thickness (symmetric slab), cm
m = weight of the sample, g
$\dot{m}$ = overall drying rate, g/s
P = total pressure, mmHg
P^w = partial pressure of water vapor, mmHg
Q = heat flux, cal/s-cm^2
S = normalized interface position
t = process time, s
T = temperature, °K
V = volume, cm^3
W = effective mass flux of water vapor, g/s-cm^2
x_w = initial moisture content of beef sample (wet basis)

Greek Letters

β = Biot number
δ = thickness of the dried layer, cm
ϵ' = relative dielectric constant
μ = fraction of the initial moisture content
μ' = corrected fraction of the initial moisture content defined by Equation (3)
Φ = total microwave power absorbed, cal/s

Superscripts and Subscripts

0 = initial value; before the microwave power is turned on
1 = starting value; *immediately* before the microwave power is turned on
2 = final value; as the frozen core disappears
f = final value; as the material is fully dried
D = in the dried layer
F = in the frozen region
i = at the interface
R = in the vacuum (room)
S = at the outer surface

LITERATURE CITED

Copson, D. A., "Microwave Sublimation of Foods," *Food Technol.*, 12, 270 (1958).

Gouigo, E. I., C. S. Malkhov, and E. I. Kaukhcheshvili, "Certaines Particularites du Transfert de Chaleur et de Masse aucours de la Lyophilisation de Produits Poreux dans un Champ Haute-Frequence," Inst. Intern. du Froid, Commission X, Lausanne, Switz. (1969).

Harper, J. C., "Microwave Spectra and Physical Characteristics of Fruit and Animal Products Relative to Freeze-Dehydration," QM Contract Report, DA19-129-QM-1349 (1961).

Hoover, M. W., A. Markantonatos, and W. N. Parker, "UHF Dielectric Heating in Experimental Acceleration of Freeze-Drying of Foods," *Food Technol.*, 20, 103 (1966).

———— "Engineering Aspects of Using UHF Dielectric Heating to Accelerate the Freeze-Drying of Foods," *ibid.*, 20, 107 (1966).

Jackson, S., S. L. Rickter, and C. O. Chichester, "Freeze-Drying of Fruit," *ibid.*, 11, 468 (1957).

Kan, B., and R. A. Yeaton, "Improving Freeze-Drying Process Efficiency through Improved Vapor Removed and In-Process Moisture Determination," QM Contract Report, DA 12-129-QM-1546 (1961).

Ma, Y. H., and P. Peltre, "Mathematical Simulation of a Freeze-Drying Process Using Microwave Energy," *AIChE Symp. Ser. No. 132*, 69, 47 (1973).

————., "Freeze Dehydration by Microwave Energy, Part I Theoretical Investigation," *AIChE J.*, 21, 335 (1975).

Peltre, P., "Freeze-Dehydration by Microwave Energy," Ph.D. thesis, Worcester Polytechnic Inst., Mass. (1974).

Manuscript received August 21, 1974; revision received December 26, 1974, and accepted January 2, 1975.